Surface reconstructions of cubic gallium nitride (001) grown by radio frequency nitrogen plasma molecular beam epitaxy under gallium-rich conditions

Muhammad B. Haider, Rong Yang, Costel Constantin, Erdong Lu, and Arthur R. Smith[a)]
Condensed Matter and Surface Science Program, Department of Physics and Astronomy, Ohio University, Athens, Ohio 45701

Hamad A. H. Al-Brithen
Condensed Matter and Surface Science Program, Department of Physics and Astronomy, Ohio University, Athens, Ohio 45701 and Department of Physics, King Saud University, Riyadh 11421, Saudi Arabia

(Received 26 November 2005; accepted 5 July 2006; published online 27 October 2006)

Cubic GaN has been grown under gallium (Ga)-rich growth conditions using radio frequency nitrogen plasma molecular beam epitaxy on MgO(001) substrates. Reflection high energy electron diffraction patterns indicate the smoothness of the *c*-GaN surface and show 2× and even 8× periodicities after the growth at sample temperature $T_s < 200\ ^\circ\mathrm{C}$ and 1×1 at higher temperatures. Scanning tunneling microscopy images reveal a sequence of variant surface reconstructions including *c*(4×12), 4×7, *c*(4×16), 4×9, *c*(4×20), and 4×11. These variant reconstructions correspond to slightly different Ga adatom coverages all less than 1/4 ML, with 4×11 having the highest, and *c*(4×12) the lowest Ga coverage. The electronic properties of these six variant reconstructions are investigated, and they are found to have a metallic nature. © *2006 American Institute of Physics*. [DOI: 10.1063/1.2356604]

I. INTRODUCTION

The topic of cubic GaN has attracted and received much attention due to the direct wide band gap and tetrahedral zinc-blende bonding structure, which could lead to the growth of GaN alloys and heterostructures with other tetrahedral zinc-blende structure semiconductors.[1–12]

A number of different atomic reconstructions have been observed on *c*-GaN(001), depending on the growth conditions and the substrate. For growth of *c*-GaN on GaAs(001), 1×1, 2×2, and *c*(2×2) reconstructions were reported.[4–7] A $\sqrt{10}\times\sqrt{10}-R$ 18.4° reconstruction was also reported.[1,2]

The growth of *c*-GaN(001) on SiC/Si(001), by contrast, resulted in 1×1 and 4×1 reconstructions which are correlated with the sample temperature and the Ga flux during growth.[6–10] However, when an arsenic background was applied, the surface showed an irreversible transition to 2×2 under slight N-rich conditions and an irreversible transition to *c*(2×2) at near-stoichiometric conditions.[9,10]

A recent study by Kim *et al.* showed that under Ga-rich conditions, growth of GaN on GaP(001) leads to single crystal *c*-GaN with a 2×2 surface reconstruction. However, under N-rich growth conditions, a wurtzite GaN layer grew preferentially.[11]

Kikuchi *et al.* described the growth of GaN on MgO(001), and they reported a 1×1 reconstruction.[6] Moreover, Powell *et al.* reported that the surface of *c*-GaN on MgO(001) had a two-domain 4×1 structure when the growth temperature was above 600 °C.[12]

Neugebauer *et al.*, by employing first principles total energy calculations, reported that 4×1, consisting of linear Ga tetramers, is the intrinsic reconstruction, whereas 2×2 is an arsenic-stabilized reconstruction.[3] Neugebauer *et al.* found that 2×2 is stable if the reconstruction involves As adatoms, and similar behavior is expected for the other group V surface adatoms, in agreement with the 2×2 reconstruction reported for *c*-GaN grown on GaAs(001) and GaP(001).

Here, we present scanning tunneling microscopy (STM) images of a group of variant surface reconstructions found on the Ga-rich-grown GaN(001) on MgO(001) substrate. We have deduced that these variant reconstructions are composed of Ga adatoms. Our molecular beam epitaxy (MBE) growth of *c*-GaN(001) on MgO(001) takes place in an ultrahigh vacuum (UHV) chamber free of arsenic and phosphor, and hence the reconstructions presented here on *c*-GaN(001) are not derived from any such group V impurities on the surface. Moreover, we have not observed any 2×2 reconstructions, which, according to Neugebauer *et al.*, are formed by As or other group V adatoms on the *c*-GaN(001) surface. The variant reconstructions presented here differ slightly from each other in terms of Ga coverage and are intrinsic reconstructions of clean *c*-GaN(001) surface. The Ga adatom coverage of these Ga-rich reconstructions varies by only ~9% and is always less than 1/4 monolayers (ML). Finally, scanning tunneling spectroscopy (STS) has been employed to determine the electronic properties of the surface reconstructions.

II. EXPERIMENTAL PROCEDURE

Growth is performed in a custom designed ultrahigh vacuum MBE chamber, whereafter the samples can be transferred to an UHV analysis chamber for room temperature

a)Author to whom correspondence should be addressed; electronic mail: smitha2@ohio.edu

 © 2006 American Institute of Physics

Downloaded 31 Oct 2006 to 132.235.26.89. Redistribution subject to AIP license or copyright, see http://jap.aip.org/jap/copyright.jsp

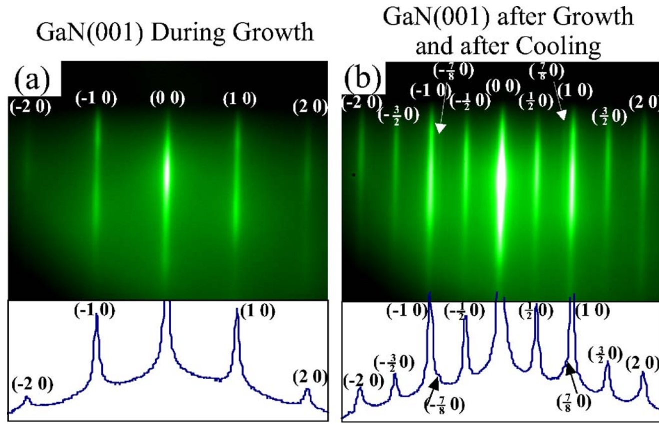

FIG. 1. (Color online) RHEED patterns for (a) c-GaN(001) during growth and (b) c-GaN(001) after growth below 200 °C. Corresponding line profiles for each image are also displayed.

STM studies without exposing the samples to air. Substrates are chemically cleaned with acetone and isopropanol before introducing them into the UHV chamber.[13,14] Cubic GaN(001) layers are grown on MgO(001) substrates using a (rf) N-plasma source and an effusion cell for gallium. GaN growth takes place with the substrate temperature set in the range of ~550–700 °C and the base pressure of nitrogen and plasma source power set at $0.9-1.1\times10^{-5}$ Torr and 500 W, respectively. The growth is monitored in real time using reflection high energy electron diffraction (RHEED).

The growth starts when the Ga shutter is opened. The Ga flux is determined using a crystal thickness monitor held at 20 °C. Gallium rich growth conditions occur at a certain threshold of Ga flux, which depends on the N flux. The Ga-rich growth conditions occur in our system at a Ga flux of $\sim3\times10^{14}/\text{cm}^2$ s. The growth is ended by closing the Ga shutter and turning off the plasma power simultaneously. So the surface studied is *as-grown* without further modification.

III. RESULTS AND DISCUSSION

A. Surface structure

1. Reciprocal Space Investigations

Shown in Fig. 1 are the RHEED patterns and their horizontal line profiles for the GaN(001) film along ⟨110⟩ of MgO(001). Shown in Fig. 1(a) is the RHEED pattern of the GaN film during the growth. Shown in Fig. 1(b) is the RHEED pattern after the growth and after cooling to below 200 °C. The GaN(001) RHEED patterns show the same structure at 90° increments around the surface normal, a consequence of the fourfold symmetry of the MgO substrate.

In Fig. 1(a), the streaky 1×1 RHEED pattern of c-GaN(001) grown under Ga-rich growth conditions shows that the surface is grown smoothly. After growth, the RHEED pattern also shows similar 1×1 structure at temperatures $T_s>200$ °C. The ratio of the spacing between the main streaks for MgO(001) to that for c-GaN(001) equals the inverse ratio of their lattice constants, $(a_{\text{MgO}}/a_{c\text{-GaN}})^{-1}$. This indicates that ⟨110⟩ of c-GaN(001) are parallel to ⟨110⟩ of MgO(001).

After the sample is cooled below 200 °C, the RHEED pattern of c-GaN(001) along [110] shows 1/2-order and 7/8-order diffraction streaks, as can be seen in the line profile of Fig. 1(b). If the sample temperature is raised above 200 °C, the RHEED pattern will again show only first-order streaks, suggesting a reversible behavior. Since the growth was under Ga-rich conditions, it may be assumed that above 200 °C, the surface contains a lot of Ga adatoms diffusing across the otherwise 1×1 unreconstructed surface. The question is then what sort of surface structures exist on c-GaN(001) at temperatures below ~200 °C when those Ga adatoms condense. We will show later by STM images that the surface at room temperature is composed of a group of variant reconstructions having periodicities of 6×, 7×, 8×, 9×, 10×, and 11×. Most likely, the coexistence of this group of variant structures having periodicities in the range of 6–11 is responsible for effectively canceling out almost all of the higher-order diffraction lines in RHEED since the surface does not have a consistent periodicity.

The coexistence in RHEED of the 1/2-order and 7/8-order streaks indicates the simultaneous sampling of 2 × and ~8× periodicities. As we will show, these periodicities are orthogonal to each other for each of the variant reconstructions observed. Why we see them both in the same RHEED pattern is simply because the substrate MgO(001) has fourfold symmetry, whereas *zinc-blende* GaN(001) has only twofold symmetry. This leads to the nucleation of two types of cubic domains on the substrate surface which are related to each other by a 90° rotation. RHEED, sampling an area of hundreds of micrometers at once, will therefore obtain a pattern having lines related to the two orthogonal crystallographic directions—[110] and $[1\bar{1}0]$.

The 2× periodicity we find for the intrinsic, clean surface is different from any previously reported 2× reconstructions which occur when using GaAs(001) or GaP(001) substrates, or when having an arsenic background for SiC(001) substrates.[1,2,5,7,9,11] This is because, first of all, As and P are avoided in our case by using MgO(001) as a substrate and our chamber is free of any other group V elements or compounds other than N. Second, the 2× periodicity observed for our sample does not occur during the growth or even at sample temperatures higher than 200 °C, whereas the previously reported 2× reconstructions did occur even during growth. Third, the 2× observed in this work below 200 °C is associated with a larger periodicity (6×–11×) in the orthogonal direction, whereas previously reported 2× structures are quite different.

Since we grow the c-GaN(001) under Ga-rich conditions, it is expected to have excess Ga on the surface. Moreover, due to the order-disorder transition observed at T_s ~200 °C, it can be inferred that Ga adatoms on a Ga-*terminated* (but neither N-nor Ga-polar) c-GaN(001) surface are responsible for forming the condensed reconstructions [note that zinc-blende(001) surfaces do not have polarity].

Comparing c-GaN(001) reconstructions with wurtzite (w)-GaN$(000\bar{1})$ surface reconstructions is helpful to understand the reversibility of these Ga adatom reconstructions. Smith *et al.* reported the formation of 3×3 Ga adatom re-

Downloaded 31 Oct 2006 to 132.235.26.89. Redistribution subject to AIP license or copyright, see http://jap.aip.org/jap/copyright.jsp

constructions on a 1×1 Ga adlayer for *w*-GaN$(000\bar{1})$ grown by rf N-plasma MBE under Ga-rich growth conditions.[15] The 3×3 reconstruction formed at $T_s \leq 300$ °C, and it was associated with a reversible order-disorder phase transition of the Ga adatoms atop the 1×1 Ga adlayer. Also higher-order reconstructions with order-disorder transitions were reported by Smith *et al.* for *w*-GaN$(000\bar{1})$ for higher Ga coverage, including 6×6 and $c(6\times12)$ reconstructions. These reversible order-disorder transitions were attributed to weak Ga–Ga bonding between the Ga adatoms and the Ga adlayer compared to the stronger Ga–N bonding. This suggests that the group of variant reconstructions observed on *c*-GaN(001) as presented here may also be composed of Ga adatoms.

To explore this, we have also manipulated the amount of Ga on the *c*-GaN(001) surface. We previously reported the formation of the 4×3 "tetramer" reconstruction on *c*-GaN(001) by annealing the sample at 740 °C, which resulted in the removal of all the Ga adatoms.[16] We reported that the 4×3 structure (*not* an adatom reconstruction) is semiconducting with a band gap of about 1.14 eV. We have also performed Ga deposition experiments onto this tetramer 4×3 surface; we found that the $4\times$ streaks disappeared and characteristic 1/2-order streaks of the $2\times$ surface reappeared after depositing only 0.1 ML of Ga. Similar behavior as seen here for *c*-GaN(001) was also observed previously in the case of *w*-GaN$(000\bar{1})$, where annealing the 3×3 reconstruction removes the Ga adatoms and leads to 1×1 reconstruction.[15]

2. Scanning tunneling microscopy studies

STM studies were performed to investigate the *c*-GaN(001) surface reconstructions in real space. Shown in Figs. 2(a)–2(d) are some large scale STM images of the Ga-rich grown *c*-GaN(001). Shown in Fig. 2(a) is a STM image of size 2200×2200 Å^2 (V_S=+2 V, I_t=0.08 nA). The surface consists of a terrace-step structure. The terraces are atomically smooth and the step height is about 2.1 Å. Shown in Fig. 2(b) is a zoom-in STM image of size 1200×1200 Å^2 (V_S=+2 V and I_t=0.08 nA). The steps appear more clearly in this image, and some rowlike features can be seen on the surface. Shown in Figs. 2(c) and 2(d) are STM images of yet smaller zoom-in areas of the surface with sizes of 450×450 Å^2 and 600×600 Å^2 (V_S=+1.5 and +2 V, respectively; I_t=0.08 nA). These images both show rowlike structure on the surfaces, and one can clearly see dislocations, vacancies, and steps. We find that similar row-type structures, such as seen here, are found everywhere on the surface, in two different domains at 90° with respect to each other.

Shown in Fig. 3(a) is a STM image (V_S=−0.4 V and I_t=0.1 nA) of *c*-GaN(001) showing the rowlike structure with atomic resolution. The rows consist of atoms arranged in various types of surface reconstructions. In this STM image, there appear three different reconstructions: $c(4\times12)$, 4×7, and $c(4\times16)$. Schematic models of these three reconstructions are presented in Figs. 3(b)–3(d), where large dots represent Ga adatoms (first layer) and small dots represent the underlying Ga atoms (second layer). Wavy lines delineate the various rows.

The $c(4\times12)$ reconstruction shown in the STM image of Fig. 3(a) consists of row structures having a periodicity along $[1\bar{1}0]$ of 19.2 Å=$6a$, where a=3.20 Å=$a_o/\sqrt{2}$, with a_o=4.53 Å—the cube-edge lattice constant of *c*-GaN. Each row structure consists of two alternating linear groups of three and two Ga adatoms [aligned (3,2) sequence] aligned perpendicular to the [110] row direction. The Ga adatoms themselves occupy every other available site with a spacing between adatoms of $2a$=6.40 Å. The spacing between these linear groups along [110] is also $2a$. This $2\times$ periodicity was observed in the RHEED pattern shown in Fig. 1(b). Due to the alternating (3,2) sequence, the repeat period along [110] is $4a$. Moreover, the spacing between the last Ga adatom in one row and the first Ga adatom in the adjacent row along $[1\bar{1}0]$ is $3a$=9.6 Å. This $3a$ spacing between groups from adjacent rows is observed for all the reconstructions presented here. From the symmetry and measured atomic spacings of the row structure, a structural model is deduced as presented in Fig. 3(b). Each $c(4\times12)$ unit cell consists of ten Ga adatoms within an area of 48 primitive 1×1 units, which corresponds to a Ga adatom coverage Θ=10/48 =0.208 ML.

As seen in the STM image of Fig. 3(a), the 4×7 structure also consists of linear groups of three Ga adatoms which shift back and forth by one primitive lattice site between two positions as one moves along the [110] row direction [zigzag (3,3) sequence]. Again, the spacing between Ga adatoms within the groups is $2a$ and the spacing between groups in adjacent rows is $3a$, whereas the spacing and repeat period for groups along [110] are $2a$ and $4a$, respectively. As seen from the structural model of Fig. 3(c), 4×7 rows are therefore separated by $7a$=22.4 Å along $[1\bar{1}0]$, and one 4×7 unit cell contains six Ga adatoms within an area of 28 primitive 1×1 units, resulting in Θ=6/28=0.214 ML.

Also seen in Fig. 3(a) is the $c(4\times16)$ structure. This structure is similar to both the $c(4\times12)$ and 4×7, but instead consists of four and three adatom linear groups which alternate along the [110] row direction [aligned (4,3) sequence]. As with the previous structures, the spacing between adatoms within a group along $[1\bar{1}0]$ as well as the spacing between groups along [110] are both $2a$. The separation between groups from adjacent rows is also $3a$, while the repeat period along [110] is also $4a$. Therefore the spacing between row centers is $8a$, but the repeat period along $[1\bar{1}0]$ is $16a$. The schematic model for the $c(4\times16)$ reconstruction is presented in Fig. 3(d). Based on the model, Θ =14 adatoms/64 primitive 1×1 unit cells=0.219 ML.

Shown in Figs. 4(a) and 4(b) are the STM image (V_S= −0.4 V; I_t=0.1 nA) and schematic atomic model of the 4×9 reconstruction, which consists of linear groups of four Ga adatoms. These groups shift back and forth between two positions offset from each other by one primitive lattice site (similar to the 4×7) as one moves along the [110] row direction [zigzag (4,4) sequence]. Again, the spacing between Ga adatoms within linear groups, as well as the spacing be-

Downloaded 31 Oct 2006 to 132.235.26.89. Redistribution subject to AIP license or copyright, see http://jap.aip.org/jap/copyright.jsp

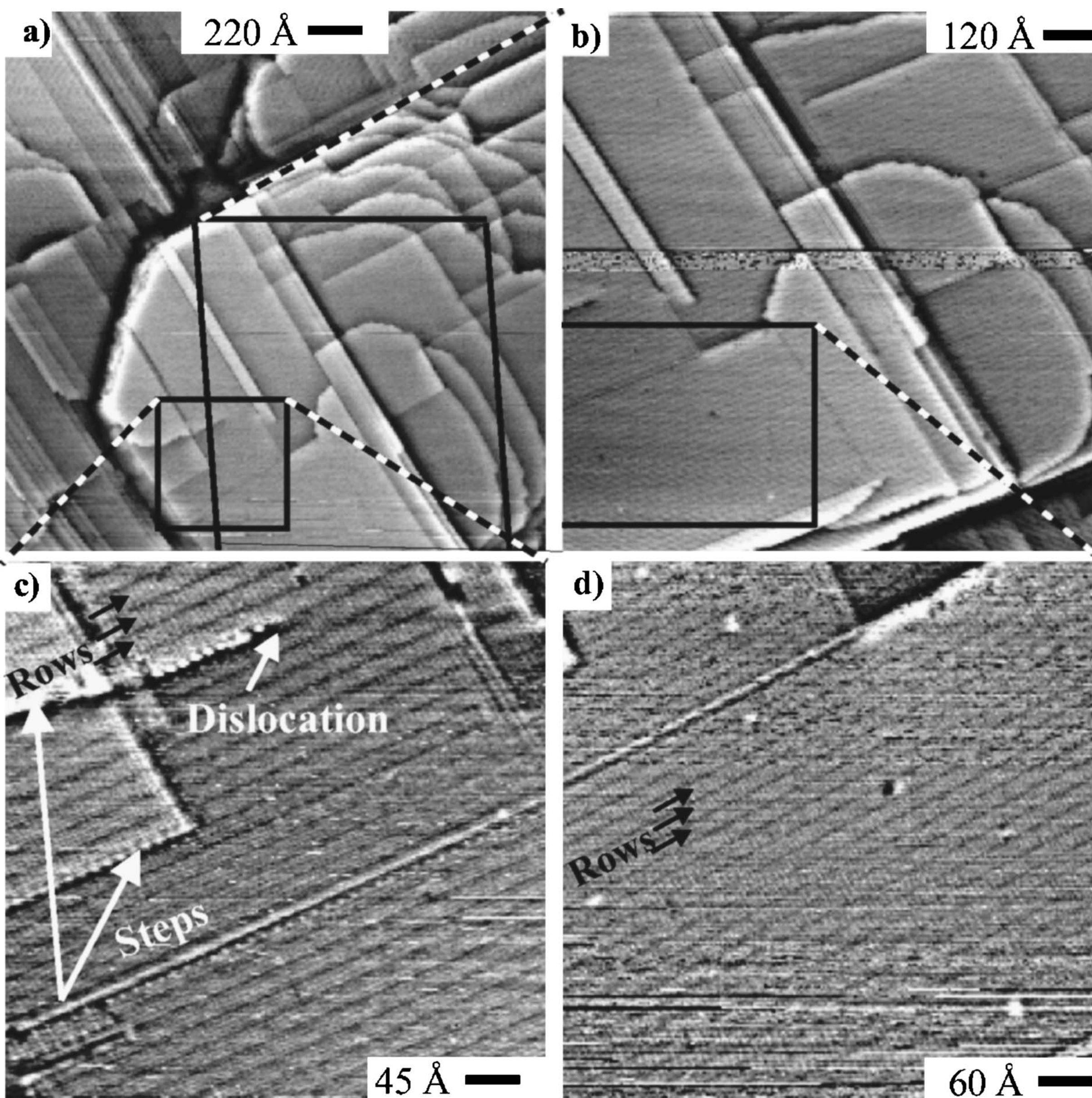

FIG. 2. STM images of c-GaN(001) surface: (a) large scale image with nominal area$=2200\times2200$ Å^2, $V_S=+2$ V; (b) zoom-in of boxed region with nominal area$=1200\times1200$ Å^2, $V_S=+2$ V; (c) small zoom-in with nominal area$=450\times450$ Å^2, $V_S=+1.5$ V; and (d) small zoom-in with nominal area$=600\times600$ Å^2, $V_S=+2$ V. For each image, $I_t=0.08$ nA.

tween linear groups along [110], is $2a$. The separation between linear groups along [$1\bar{1}0$] is $3a$. And the periodicities along [110] and along [$1\bar{1}0$] are $4a$ and $9a$, respectively [see model in Fig. 4(b)]. Looking very closely at the STM image, it can be noticed that the corrugation within a linear group is not exactly even; the adatoms at the furthest outer edge positions for a given [110] row are brighter (in grayscale) compared with their neighbors, and then the adatom second from the end has the same brightness as the brighter end adatom. This subtle effect suggests a slight buckling of the substrate atoms or else a slight redistribution of the density of filled states. Such a symmetrical redistribution could be the result of a degeneracy-lifting effect mediated by a slight charge separation. There are eight Ga adatoms for each 4×9 unit cell equal to 36 primitive 1×1 unit cells, leading to $\Theta=8/36=0.222$ ML.

Shown in Figs. 5(a) and 5(b) are STM image ($V_S=-0.4$ V, $I_t=0.1$ nA) and schematic atomic model for the next Ga-rich reconstruction, the $c(4\times20)$. Similar to the previous structures, the $c(4\times20)$ consists of rows of five and four adatom linear groups which alternate as one moves along the [110] row direction [aligned (5,4) sequence]. The spacing between adatoms within a group, as well as the spacing between linear groups along the [110] direction, is $2a$. The separation between linear groups along [$1\bar{1}0$] is $3a$, while the spacing between rows is $10a$. Moreover, the periodicities along the [110] row direction and along [$1\bar{1}0$] are $4a$ and $20a$, respectively [see model in Fig. 5(b)]. As with the 4×9 reconstruction, the $c(4\times20)$ shows a slightly uneven brightness (gray scale) for adjacent adatoms within a group, which may indicate a slight degeneracy lifting. Each c(4

Downloaded 31 Oct 2006 to 132.235.26.89. Redistribution subject to AIP license or copyright, see http://jap.aip.org/jap/copyright.jsp

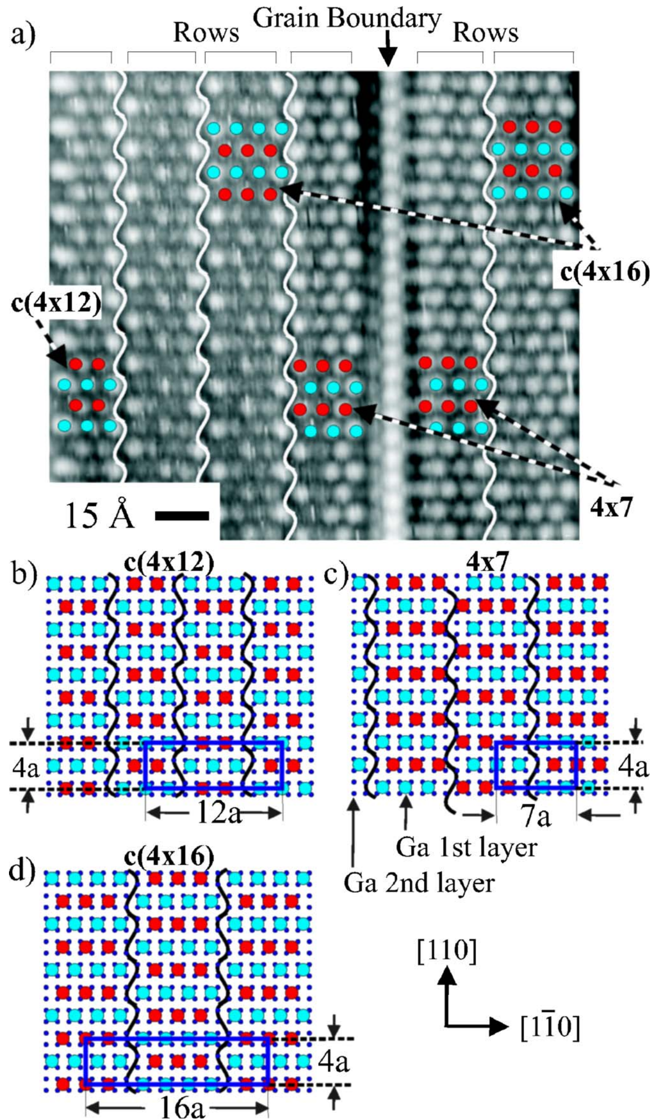

FIG. 3. (Color online) STM image (a) of c-GaN(001) Ga-rich, mixed reconstructions $c(4\times12)$, 4×7, and $c(4\times16)$, with $V_s=-1.5$ V and $I_t=0.07$ nA; and schematic atomic models of (b) $c(4\times12)$, (c) 4×7, and (d) $c(4\times16)$. The wavy lines delineate the different reconstruction rows (Both red and aqua blue large dots are first-layer Ga adatoms, while dark blue small dots are second-layer Ga atoms).

$\times20)$ unit cell contains 18 Ga adatoms within an area equivalent to 80 primitive 1×1 unit cells, resulting in $\Theta=18/80=0.225$ ML.

A STM image ($V_S=-1$ V, $I_t=0.1$ nA) and schematic atomic model of the next reconstruction in this series—the 4×11—are shown in Figs. 6(a) and 6(b). The 4×11 consists also of rows of Ga adatom linear groups, in this case of five adatom groups which shift back and forth by one primitive lattice site [zigzag (5,5) sequence] as one moves along the [110] row direction. Once again, the spacing between adatoms within a group, as well as the spacing between groups along the [110] direction, is $2a$. The separation between groups along $[1\bar{1}0]$ is $3a$, and in the ideal model the repeat distances along [110] and along $[1\bar{1}0]$ are $4a$ and $11a$, respectively. The adatoms at the row edges (one end of each five adatom groups) appear brighter (gray scale) compared to the other adatoms in the group. There are ten Ga adatoms in

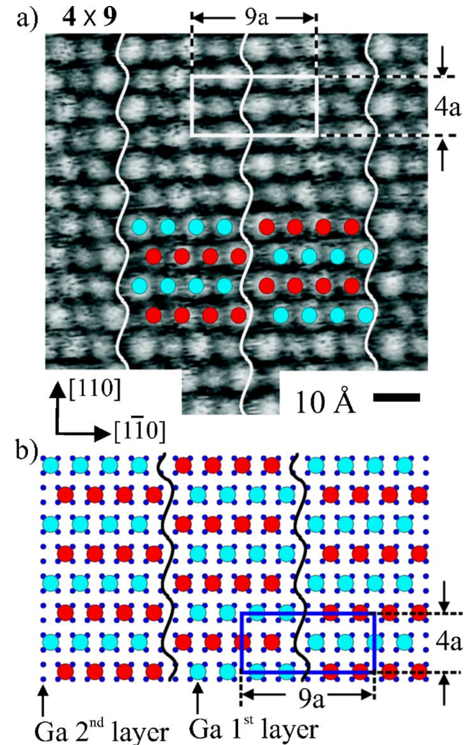

FIG. 4. (Color online) STM image (a) of c-GaN(001)-4×9 reconstruction variant acquired at $V_s=-0.8$ V and $I_t=0.07$ nA, and (b) schematic model of 4×9. The wavy lines delineate 4×9 rows (Both red and aqua blue large dots are first-layer Ga adatoms, while dark blue small dots are second-layer Ga atoms).

each 4×11 unit cell equivalent to an area of 44 primitive 1×1 unit cells, giving $\Theta=10/44=0.227$ ML.

3. Variants of a single adatom phase

Based on the foregoing discussion, we have observed and presented six closely related Ga adatom reconstructions

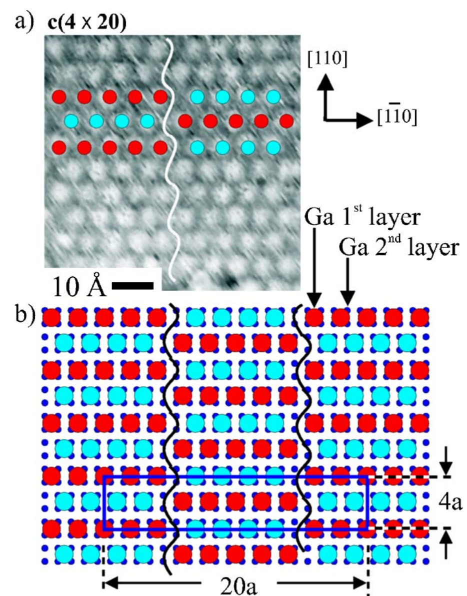

FIG. 5. (Color online) STM image (a) of c-GaN(001)-$c(4\times20)$ variant acquired at $V_s=-0.4$ V and $I_t=0.1$ nA, and (b) schematic model of $c(4\times20)$. The wavy lines delineate $c(4\times20)$ rows (Both red and aqua blue large dots are first-layer Ga adatoms, while dark blue small dots are second-layer Ga atoms).

Downloaded 31 Oct 2006 to 132.235.26.89. Redistribution subject to AIP license or copyright, see http://jap.aip.org/jap/copyright.jsp

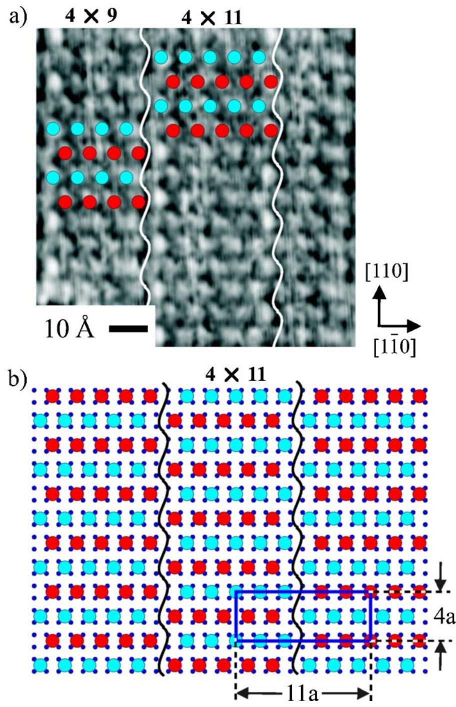

FIG. 6. (Color online) STM image (a) of c-GaN(001) mixed 4×11 and 4×9 variants acquired at $V_s=-1.0$ V and $I_t=0.1$ nA and (b) schematic model of 4×11. The wavy lines delineate different variant rows (Both red and aqua blue large dots are first-layer Ga adatoms, while dark blue small dots are second-layer Ga atoms).

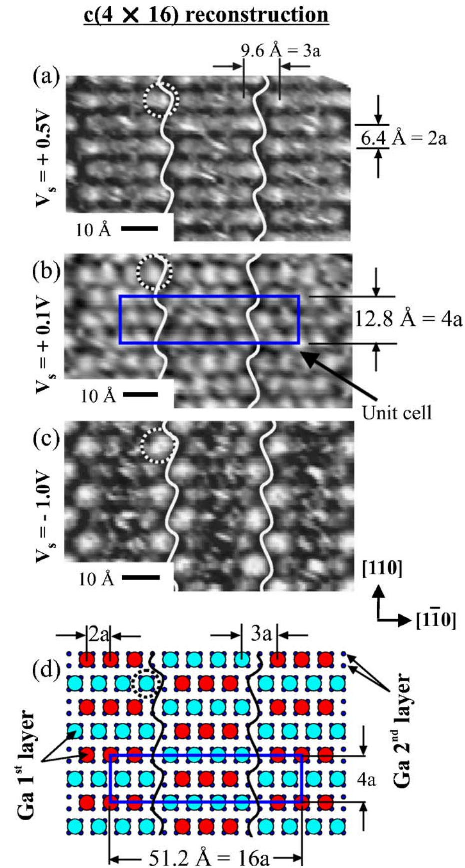

FIG. 7. (Color online) STM images of c-GaN(001)-$c(4\times16)$ acquired at different sample biases and tunneling currents: (a) $V_s=+0.5$ V, $I_t=0.6$ nA; (b) $V_s=+0.1$ V, $I_t=0.9$ nA; and (c) $V_s=-1.0$ V, $I_t=0.2$ nA. Gray scales corresponding to (a), (b), and (c) are 0.82, 0.96, and 1.43 Å, respectively. (d) schematic model of $c(4\times16)$. The wavy lines delineate $c(4\times16)$ rows (Both red and aqua blue large dots are first-layer Ga adatoms, while dark blue small dots are second-layer Ga atoms).

together with schematic atomic models, corresponding to the clean c-GaN(001) surface: $c(4\times12)$, 4×7, $c(4\times16)$, 4×9, $c(4\times20)$, and 4×11. These reconstructions are really just variants of a single adatom phase which condenses at temperature $T\leqslant200$ °C, well below the typical GaN growth temperature, and becomes disordered if the temperature is raised. It is worth noting that the progression of Ga coverage (see Table I), beginning at $\Theta=0.208$ ML $[c(4\times12)]$ and going up to $\Theta=0.227$ ML $[4\times11]$ is a trend with an ultimate end point. For example, if the rows become wider and wider (e.g., imagine $4\times n$ with $n\rightarrow$ very large), the average coverage Θ will approach that *within* any row $\Theta_{\text{row}}=1/4$ ML. At exactly $\Theta=1/4$ ML, there would be no rows and the surface would consist only of $c(4\times2)$ reconstruction.

One may then question why the surface adopts these large $4\times n$ and $c(4\times m)$ reconstructions with various n and m rather than a simple $c(4\times2)$ from the beginning. We assume that strain does not play a role since the minimum spacing between Ga adatoms is 6.4 Å, much larger than the typical 2.7 Å spacing between Ga atoms in bulk Ga metal and therefore too large to allow significant Ga–Ga interadatom bonding. One possibility is that the surface can better satisfy electron counting by opening up lines of half-filled second-layer Ga atom dangling bonds. However, as we show in the next section, this surface is metallic, and it is well known for metallic surfaces that it is not necessary to satisfy electron counting. Furthermore, we also show below that while there are clear differences between empty and filled state STM images (bias voltage dependence), the adatom linear groups have both filled and empty states (whereas for a semiconducting surface, electron counting usually means that the surface states are either completely filled or completely empty). Thus we leave it for future work to explain the stability of these large unit cell variant reconstructions.

TABLE I. Intrinsic c-GaN(001) Ga-rich $4\times n$ and $c(4\times m)$ variant reconstructions with their various properties.

Reconstruction	Variant squence	Row spacing	Ga adatom coverage (ML)
$c(4\times12)$	Aligned (3,2)	$6a$	0.208
4×7	Zigzag (3,3)	$7a$	0.214
$c(4\times16)$	Aligned (4,3)	$8a$	0.219
4×9	Zigzag (4,4)	$9a$	0.222
$c(4\times20)$	Aligned (5,4)	$10a$	0.225
4×11	Zigzag (5,5)	$11a$	0.227

B. Electronic properties

1. Bias voltage-dependent STM images

To gain information about the electronic structure of the surface, STM images were obtained as a function of bias voltage. The bias-voltage-dependent structure of the $c(4\times16)$ is shown in Figs. 7(a)–7(c) with the corresponding surface model shown in Fig. 7(d). At sample bias voltage $V_S=+0.5$ V [Fig. 7(a)], the corrugation within the four and

Downloaded 31 Oct 2006 to 132.235.26.89. Redistribution subject to AIP license or copyright, see http://jap.aip.org/jap/copyright.jsp

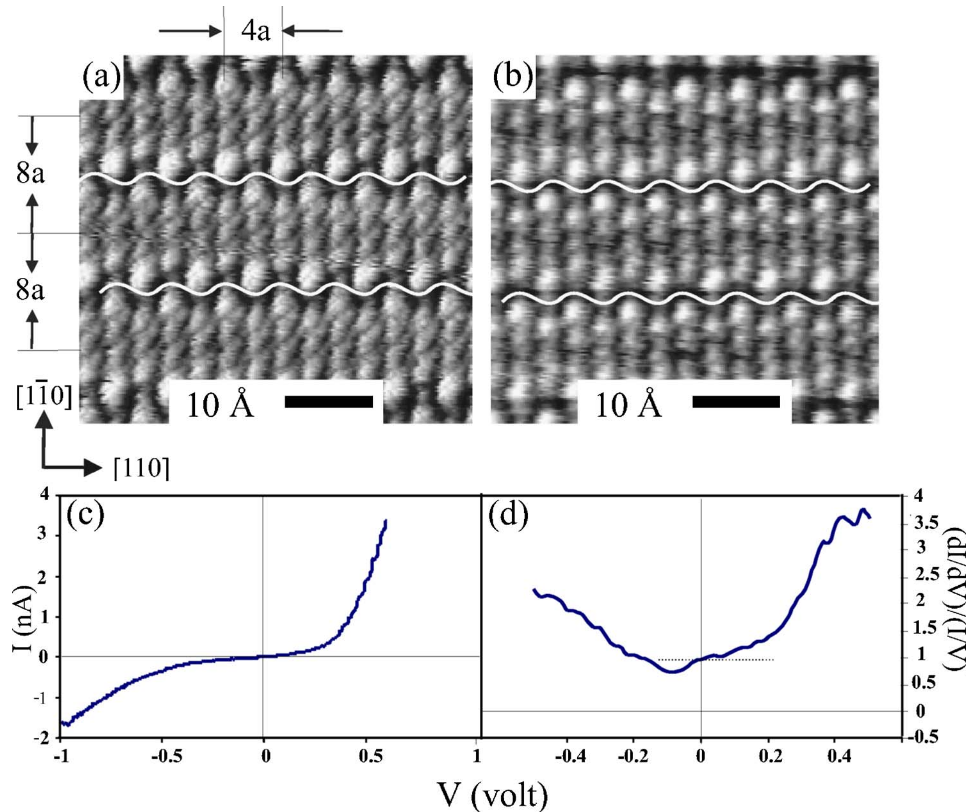

FIG. 8. (Color online) STM and STS of c-GaN(001)-$c(4\times16)$ reconstruction: [(a) and (b)] STM images acquired at $V_s=+0.3$ and -0.3 V, respectively, with the same tunneling current, $I_t=0.08$ nA; (c) tunneling current vs voltage (I-V) curve; and (d) normalized conductivity vs voltage (NC-V) curve.

three adatom linear groups for empty states is very weak, giving these adatom groups the appearance of short and long segments, with the adatoms themselves being indistinct. But at very small positive sample bias $V_S=+0.1$ V [Fig. 7(b)], the corrugation within the groups is much stronger, and the individual adatoms appear distinct. Then at sample bias $V_S=-1$ V, corresponding to filled states of the sample, the outer two adatoms of the linear groups are fairly distinct, whereas the inner adatoms are indistinct [Fig. 7(c)].

Therefore, there are clearly some differences in the state filling for different adatoms. However, since the adatoms appear as peaks in both empty and filled states, the surface is not semiconducting but rather metallic. This conclusion is consistent with a surface consisting of weakly bound Ga adatoms atop the Ga atoms of the outermost Ga–N bilayer.

2. Scanning tunneling spectroscopy

Further information about the electronic structure of the Ga-rich surface is shown in Fig. 8, including [(a) and (b)] STM images of c-GaN(001)-$c(4\times16)$ reconstruction, (c) tunneling current versus voltage (I-V) spectroscopy obtained using STS on the same area, and (d) the numerically derived normalized conductance $(dI/dV)/(\overline{I/V})$ versus voltage (NC-V). The bar over the I/V indicates that broadened I/V values are used to avoid divergence near the band edges.[17] We have used a broadening of 0.05 V. Both I-V and NC-V curves are the averages of 16 individual spectra.

The sample bias voltages for the STM images of the $c(4\times16)$ reconstruction shown in Figs. 8(a) and 8(b) are +0.3 V (empty states) and −0.3 V (filled states), respectively. Consistent with the results from Fig. 7, the atomic corrugation has the same polarity for both empty and filled states at the same location on the surface (no polarization reversal), consistent with metallic surface states. Furthermore, the fact that STM images were obtained for very small bias voltage magnitudes implies that there must be either very small or zero surface band gap.

The STS results further prove the nature of the electronic properties of the Ga-rich c-GaN(001) $c(4\times16)$ surface. As seen in Fig. 8(c), the tunneling current smoothly increases (decreases) as the bias voltage V_S increases (decreases) away from zero volt. There is no apparent band gap to the resolution of the I-V graph presented; in fact, the I-V curve near 0 V appears to have a linear region, which suggests a constant density of states (DOS) near the Fermi level.

To be even more conclusive, as shown in Fig. 8(d), the normalized conductance—a quantity known to be proportional to the DOS—shows a broad valley of states lying between −0.5 and +0.5 V. The state density never goes to zero, reaching the (normalized) value of 1 at 0 V (sample bias) and ~0.75—the minimum point—at ~−0.09 V. Therefore, there is definitely no band gap (to the available resolution) for this Ga-rich c-GaN(001) surface structure composed of Ga adatoms on top of the Ga-terminated GaN(001) surface.

The result can be extended to all of the six variants of the Ga adatom reconstruction presented here. Since these six structures are actually almost equivalent, given that their Ga coverages Θ are nearly the same, and more importantly that the reconstruction of each of them is really just $c(4\times2)$ divided into rows, or strips with spacing of 6–11 primitive units, we can realize that the electronic properties presented in Fig. 8 for the $c(4\times16)$ specifically will be applicable to all six of these different variants. Furthermore, this extrapolation to the different variants is confirmed by other data, for

Downloaded 31 Oct 2006 to 132.235.26.89. Redistribution subject to AIP license or copyright, see http://jap.aip.org/jap/copyright.jsp

example, the fact that these other variant structures can also be imaged at very small magnitudes of bias voltage V_S also suggests that they have zero band gap. Therefore, we can conclude with certainty that the six variant reconstructions presented here, each having a Ga adatom coverage Θ slightly less than 1/4 ML, are metallic in nature. Nonetheless, there are still variations in the state density from point to point (adatom to adatom) on the surface, as determined by the bias-dependent STM images.

IV. SUMMARY

Cubic GaN(001) has been grown smoothly under Ga-rich growth conditions on MgO(001) using rf N-plasma MBE. A group of variant reconstructions, including $c(4\times12)$, 4×7, $c(4\times16)$, 4×9, $c(4\times20)$, and 4×11, with corresponding Ga adatom coverages $\Theta=0.208$, 0.214, 0.219, 0.222, 0.225, and 0.227 ML, respectively, was observed on Ga-rich grown *c*-GaN(001). All these six variants are shown to be composed, in fact, of a simple $c(4\times2)$ structure ($\Theta=1/4$ ML) divided into rows or strips with separation distance of 6–11 primitive units. The electronic properties of these six variant Ga adatom reconstructions have been discussed; a metallic nature of the surface structure has been found, as proven from both STM imaging and STS spectroscopy. Furthermore, due to the fact that our MBE chamber is free of other group V elements such as arsenic or phosphor, which could modify dramatically the surface structures as found historically from earlier studies by different groups, we can be sure that the variant reconstructions presented here belong to the family of intrinsic reconstructions of the clean surface of *c*-GaN(001).

ACKNOWLEDGMENTS

The material presented here is based upon work supported by the National Science Foundation under Grant Nos. 9983816 and 0304314. Support is also acknowledged from the Office of Naval Research Grant No. N00014-99-1-0528.

[1] M. Wassermeier, A. Yamada, H. Yang, O. Brandt, J. Behrend, and K. H. Ploog, Surf. Sci. **385**, 178 (1997).
[2] M. Wassermeier, H. Yang, O. Brandt, A. Yamada, J. Behrend, and K. H. Ploog, Appl. Surf. Sci. **123/124**, 181 (1998).
[3] J. Neugebauer, T. Zywietz, M. Scheffler, J. E. Northrup, and C. G. Van de Walle, Phys. Rev. Lett. **80**, 3097 (1998).
[4] S. Strite, J. Ruan, Z. Li, A. Salvador, H. Chen, D. J. Smith, W. J. Choyke, and H. Morkoç, J. Vac. Sci. Technol. B **9**, 1924 (1991).
[5] O. Brandt, H. Yang, B. Jenichen, Y. Suzuki, L. Däweritz, and K. H. Ploog, Phys. Rev. B **52**, R2253 (1995).
[6] A. Kikuchi, H. Hoshi, and K. Kishino, Jpn. J. Appl. Phys., Part 1 **34**, 1153 (1995).
[7] H. Okumura, K. Ohta, G. Feuillet, K. Balakrishnan, S. Chichibu, H. Hamaguchi, P. Hacke, and S. Yoshida, J. Cryst. Growth **178**, 113 (1997).
[8] D. Wang, S. Yoshida, and M. Ichikawa, Appl. Phys. Lett. **80**, 2472 (2002).
[9] G. Feuillet, H. Hamaguchi, K. Ohta, P. Hacke, H. Okumura, and S. Yoshida, Appl. Phys. Lett. **70**, 1025 (1997).
[10] G. Feuillet, H. Hamaguchi, H. Okumura, and S. Yoshida, Mater. Sci. Eng., B **59**, 80 (1999).
[11] M.-H. Kim, F. S. Juang, Y. G. Hong, C. W. Tu, and S.-J. Park, J. Cryst. Growth **251**, 465 (2003).
[12] R. C. Powell, N.-E. Lee, Y.-W. Kim, and J. E. Greene, J. Appl. Phys. **73**, 189 (1992).
[13] A. R. Smith, H. A. H. Al-Brithen, D. C. Ingram, and D. Gall, J. Appl. Phys. **90**, 1809 (2001).
[14] H. A. AL-Brithen and A. R. Smith, Appl. Phys. Lett. **77**, 2485 (2000).
[15] A. R. Smith, R. M. Feenstra, D. W. Greve, J. Neugebauer, and J. E. Northrup, Phys. Rev. Lett. **79**, 3934 (1997).
[16] H. A. H. Al-Brithen, R. Yang, M. B. Haider, C. Constantin, E. Lu, A. R. Smith, N. Sandler, and P. Ordejon, Phys. Rev. Lett. **95**, 146102 (2005).
[17] R. M. Feenstra, Phys. Rev. B **50**, 4561 (1994).

Downloaded 31 Oct 2006 to 132.235.26.89. Redistribution subject to AIP license or copyright, see http://jap.aip.org/jap/copyright.jsp